HEFAT2014
10th International Conference on Heat Transfer, Fluid Mechanics and Thermodynamics
14 – 16 July 2014
Orlando, Florida

TSUNAMI WAVE PROPAGATION OVER AN UNDERWATER OBSTACLE

Chugunov V.[1], Fomin S.[2]*, and Shankar R.[2]
[1]Institute of Mathematics and Mechanics, Kazan Federal University, Kazan, Russia
[2]Department of Mathematics and Statistics, California State University, Chico, CA 95929, USA
*Author for correspondence
Email: sfomin@csuchico.edu

ABSTRACT

Water wave propagation over an uneven seafloor is studied using analytical techniques in application to modeling tsunami wave dynamics on coastlines. A long, solitary wave is modeled as moving over an underwater obstacle situated on a flat seafloor. The obstruction is taken to be symmetric, rectangular, and of finite length. The linear shallow water equations are solved in the frequency domain using the method of Laplace Transforms. The solutions of regions in between the obstacle boundaries are matched together and transformed back to the time domain. The solutions to the equations demonstrate a greater variety of dynamical behavior than for the case of an obstacle of infinite length.

INTRODUCTION

The study of wave propagation over steps and underwater obstacles has numerous applications. For low cost, submerged breakwaters (underwater obstacles) offer great potential for reductions in wave erosion of beaches and wave damage to ships [1]. Study of solitary wave interaction with underwater seafloor topography provides characterization of the important tsunami-wave problem [2]. Of interest is how the incident wave amplitude is affected by ascension onto a shelf. Lamb [3] first derived the linear reflection and transmission coefficients of long waves with wavelength far greater than the water depth over an underwater shelf. His straightforward analytical results show that, for increased shelf height, the incident wave experiences greater reflection at the step. Moreover, the transmitted wave is amplified and undergoes a wavelength reduction. Focusing on monochromatic periodic waves, Lamb's results were extended and refined to short waves [4-5], the case of the underwater rectangular obstacle [6-9], an underwater trench (inverted obstacle) [10-11], and a general obstacle of trapezoidal shape [12-13]. In all cases, analysis of the more complicated seafloor with an obstacle required usage of numerical techniques or superposition of periodic solutions. An analytical solution more to the effect of Lamb [3] for wave propagation over an underwater obstacle is obtained in this study. The method of solution of the linear shallow water equations is the Laplace Transform, which is well suited for application to constant-coefficient wave equations.

NOMENCLATURE

η	vertical elevation of water from quiescent position
u	depth-averaged horizontal flow velocity
φ	distance from water surface to seafloor; water depth
φ_0	dimensional water depth of seafloor away from obstacle
φ_1	dimensional water depth of seafloor on obstacle
f	initial waveform distribution
k	dimensionless water depth on obstacle; $k^2 = \varphi_1/\varphi_0$
x	horizontal position coordinate
t	time
s	frequency domain independent variable
l	length of obstacle
d	distance of solitary wave peak from the origin $x = 0$
λ	length of the solitary wave

Subscripts

R	quantity defined in region R, $x > 0$
M	quantity defined in region M, $0 > x > -l$
L	quantity defined in region L, $x < -1$
0	characteristic dimensional quantity

Superscripts

~	function defined in frequency domain
′	dimensional variable

GOVERNING EQUATIONS AND SCALE ANALYSIS

The dynamics of small amplitude long waves with wavelength much greater than the water reservoir depth can be described by the linear shallow water equations [14]:

$$u'_{t'} + g\eta'_{x'} = 0, \quad (1a)$$

$$\eta'_{t'} + (\varphi' u')_{x'} = 0. \quad (1b)$$

Dimensional variables are given with a superscript $'$. A variable subscript denotes partial differentiation. Variable t' is time; x' is the horizontal position coordinate; $\eta'(x', t')$ is the vertical departure of the water surface from its quiescent position; $u'(x', t')$ is the depth-averaged horizontal flow velocity; g is acceleration due to gravity; $z' = -\varphi'(x')$ is the depth of the water and describes the shape of the seafloor. In this paper, we study wave run-up on an underwater rectangular obstacle of given height $\varphi_0 - \varphi_1$ and length l_0:

$$\varphi'(x') = \begin{cases} \varphi_0, & x' > 0 \\ \varphi_1, & -l_0 < x' < 0, \\ \varphi_0, & x' < -l_0 \end{cases} \quad (2)$$

where $\varphi_1 < \varphi_0$ for an obstacle and $\varphi_1 > \varphi_0$ for a trough.

We assume that the initial wave, whose profile is given by the function $f'(x')$, is generated at the initial moment of time $t' = 0$ at a distance $x' = d_0$ from the origin $x' = 0$, the point at which the sharp depth change is located. The initial wave velocity is assumed to be zero. The initial conditions for equations (1a), (1b) can be presented in the following form:

$t' = 0$: $\eta'(x', 0) = f'(x')$, (3a)

$u'(x', 0) = 0$. (3b)

Far away from the origin, the following conditions at infinity should clearly be satisfied:

$x' \to \pm\infty$: $\lim\left(\eta'(x', t') - f'(x')\right) = 0$ (4a)

$\lim u'(x', t') = 0$ (4b)

The following characteristic scales are introduced and denoted by subscript 0: η_0- characteristic wave amplitude; u_0 - characteristic fluid velocity; c_0 - characteristic velocity of wave propagation; λ_0 – characteristic length of initial wave; $t_0 = \lambda_0/c_0$ - characteristic time of propagation.

Using the above scales, nondimensional variables can be introduced as follows:

$$t = t'/t_0,\ x = x'/\lambda_0,\ \eta(x,t) = \eta'(x',t')/\eta_0,$$
$$u(x,t) = u'(x',t')/u_0,\ \varphi(x) = \varphi(x')/\varphi_0, \quad (5)$$
$$k^2 = \varphi_1/\varphi_0,\ d = d_0/\lambda_0,\ l = l_0/\lambda_0.$$

The magnitudes $\eta_0, \varphi_0, \lambda_0$ are given from the problem's conditions, so the characteristic velocity scales can be obtained from scale analysis of equations (1a), (1b):

$c_0 = \sqrt{g\varphi_0}$, $u_0 = \eta_0\sqrt{g/\varphi_0}$. (6)

After substitutions, equations (1a), (1b) become:

$u_t + \eta_x = 0$ (7a)

$\eta_t + (\varphi u)_x = 0$ (7b)

where the dimensionless seafloor depth is given by:

$$\varphi(x) = \begin{cases} 1, & x > 0 \\ k^2, & -l < x < 0, \\ 1, & x < -l \end{cases} \quad (8)$$

In new variables, the initial condition and conditions at infinity become:

$t = 0$: $\eta(x, 0) = f(x)$, (9a)

$u(x, 0) = 0$, (9b)

$x \to \pm\infty$: $\lim\left(\eta(x,t) - f(x)\right) = 0$, (10a)

$\lim u(x,t) = 0$. (10b)

To account for the discontinuous changes in seafloor depth at $x = 0$ (the step "onto" the obstacle) and at $x = -l$ (the step "down" from the obstacle), the horizontal coordinate is divided into three regions (see Fig. 1): R- to the "right" of the obstacle $0 < x$; M- the "middle" region on top of the obstacle $-l < x < 0$; L- the "left" side of the obstacle $x < -l$. It is required that equations (7), (9), (10) are satisfied in each region for function η_R, u_R and $\varphi = 1$ in region R, functions η_M, u_M and $\varphi = k^2$ in region M, and functions η_l, u_l and $\varphi = 1$ in region L.

For continuity of pressure and mass from equations (1a) and (1b) (see Lamb [3], pg. 262), conjugation conditions are imposed on the functions at $x = 0$ and $x = -l$:

$x = 0$: $\eta_M = \eta_R$; $k^2 u_M = u_R$, (11a)

$x = -l$: $\eta_L = \eta_M$; $u_L = k^2 u_M$. (11b)

Equations (7) can be decoupled into two wave equations for η and u:

$\eta_{tt} - (\varphi\eta_x)_x = 0$, (12a)

$u_{tt} - (\varphi u_x)_x = 0$. (12b)

An additional conjugation condition is imposed on the function derivatives:

$x = 0$: $k^2\eta_{Mx} = \eta_{Rx}$; $k^2 u_{Mx} = u_{Rx}$, (13a)

$x = -l$: $\eta_{Lx} = k^2\eta_{Mx}$; $u_{Lx} = k^2 u_{Mx}$. (13b)

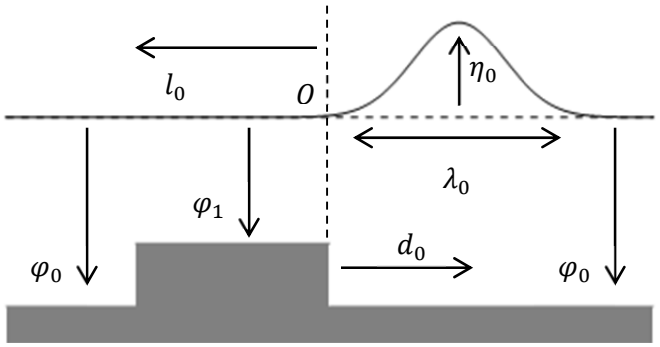

Figure 1 A schematic sketch of wave propagation over an underwater obstacle.

SOLUTION

The wave propagation in regions R, M, and L can be found by solving equations (12) in each region and matching the solutions together at $x = 0$ and $x = -l$. This has been previously done using techniques applicable to monochromatic periodic waves [12], but these solutions are not applicable to tsunami-type solitary waves. An analytical approach well suited for this type of problem is to use Laplace Transforms.

In the frequency domain, we have $\tilde{g}(x,s) = \mathcal{L}[g(x,t)] = \int_0^\infty \mathrm{e}^{-st} g(x,t)dt$, so, accounting for initial conditions (9), equations (12) become:

$\tilde{\eta}_{xx} - (s^2/\varphi)\tilde{\eta} = -(s/\varphi)f(x)$, (14a)

$\tilde{u}_{xx} - (s^2/\varphi)\tilde{u} = (1/\varphi)f'(x)$. (14b)

These equations can be readily integrated. For example, solving (14a) for $\tilde{\eta}$ gives:

$\tilde{\eta}(x,s) = \frac{1}{2\sqrt{\varphi}}\left(e^{sx/\sqrt{\varphi}}\tilde{\eta}^+(x,s) + e^{-sx/\sqrt{\varphi}}\tilde{\eta}^-(x,s)\right)$, (15a)

$\tilde{\eta}^+(x,s) = \tilde{\eta}^+(s) - \int_{L'}^{x} e^{-sy/\sqrt{\varphi}} f(y)dy$, (15b)

$\tilde{\eta}^-(x,s) = \tilde{\eta}^-(s) + \int_{L'}^{x} e^{sy/\sqrt{\varphi}} f(y)dy$, (15c)

where $y = L'$ is an appropriate lower limit of integration and $\tilde{\eta}^+(s)$, $\tilde{\eta}^-(s)$ are functions of s to be determined by conditions (10), (11). Since the determination of $\tilde{\eta}$ and $\tilde{u}$ is similar for each case, the procedure as follows is shown only for $\tilde{\eta}$.

Solutions for regions R, M, L are defined by evaluating $\varphi(x)$ for each case and setting the arbitrary integration limits $y = L'$ to $y = 0$, $y = -l$, and $y = -l$, respectively. For example, $\tilde{\eta}_M^+(x,s) = \tilde{\eta}_M^+(s) - \int_{-l}^{x} e^{-sy/k} f(y)dy$. Applying the appropriate conditions at infinity (10a) to $\tilde{\eta}_L$ and $\tilde{\eta}_R$ gives

$\tilde{\eta}_L^-(s) = \int_{-\infty}^{-l} e^{sy} f(y)dy$ and $\tilde{\eta}_R^+(s) = \int_0^{\infty} e^{-sy} f(y)dy$ for two of the six undetermined functions. Applying the conjugation conditions (11) and (13) gives a system of four linear equations for $\tilde{\eta}_L^+(s), \tilde{\eta}_M^+(s), \tilde{\eta}_M^-(s), \tilde{\eta}_R^-(s)$:

$$\frac{1}{2k}\left(\tilde{\eta}_M^+(s) + \tilde{\eta}_M^-(s) + 2\int_{-l}^{0} \sinh\left(\frac{sy}{k}\right) f dy\right) = \frac{1}{2}\left(\tilde{\eta}_R^+(s) + \tilde{\eta}_R^-(s)\right) \quad (16a)$$

$$\frac{s}{2}\left(\tilde{\eta}_M^+(s) - \tilde{\eta}_M^-(s) - 2\int_{-l}^{0} \cosh\left(\frac{sy}{k}\right) f dy\right) = \frac{s}{2}\left(\tilde{\eta}_R^+(s) - \tilde{\eta}_R^-(s)\right) \quad (16b)$$

$$\frac{1}{2}\left(e^{-sl}\tilde{\eta}_L^+(s) + e^{sl}\tilde{\eta}_L^-(s)\right) = \frac{1}{2k}\left(e^{-sl/k}\tilde{\eta}_M^+(s) + e^{sl/k}\tilde{\eta}_M^-(s)\right) \quad (16c)$$

$$\frac{s}{2}\left(e^{-sl}\tilde{\eta}_L^+(s) - e^{sl}\tilde{\eta}_L^-(s)\right) = \frac{s}{2}\left(e^{-sl/k}\tilde{\eta}_M^+(s) - e^{sl/k}\tilde{\eta}_M^-(s)\right) \quad (16d)$$

With these functions obtained from (16), we can take the inverse Laplace transform of $\tilde{\eta}(x,s)$ (15) to obtain $\eta(x,t)$. At this point, the equations become lengthy, so the computations will be illustrated only for $\tilde{\eta}_R(x,s)$. This function is found to be:

$$\tilde{\eta}_R(x,s) = \frac{1}{2}\left(e^{sx}\tilde{\eta}_R^+(x,s) + e^{-sx}\tilde{\eta}_R^-(x,s)\right), \quad (17a)$$

$$\tilde{\eta}_R^+(x,s) = \int_x^{\infty} e^{-sy} f(y)dy, \quad (17b)$$

$$\tilde{\eta}_R^-(x,s) = \tilde{\eta}_R^-(s) + \int_0^{x} e^{sy} f(y)dy, \quad (17c)$$

$$\tilde{\eta}_R^-(s) = e^{-2sl/k}\left(\sum_{j=1}^{5} a_j A_j(s)\right)/\left(\kappa_+^2 D(s)\right), \quad (17d)$$

where $\kappa_+ = 1 + k$, $\kappa_- = 1 - k$, and:

$$A_1 = e^{2sl/k}\int_0^{\infty} e^{-sy} f(y)dy;\ a_1 = \kappa_+\kappa_-, \quad (17e)$$

$$A_2 = e^{-2sl/k} A_1;\ a_2 = -a_1, \quad (17f)$$

$$A_3 = e^{2sl/k}\int_{-l}^{0} e^{sy/k} f(y)dy;\ a_3 = 2\kappa_+, \quad (17g)$$

$$A_4 = \int_{-l}^{0} e^{-sy/k} f(y)dy;\ a_4 = 2\kappa_-, \quad (17h)$$

$$A_5 = e^{sl\kappa_+/k}\int_{-\infty}^{-l} e^{sy} f(y)dy;\ a_5 = 4k, \quad (17i)$$

$$D(s) = 1 - e^{-2sl/k}(\kappa_-/\kappa_+)^2. \quad (17j)$$

Now, since $1 > k > 0$ and $s \geq 0$, the function $D(s)$ can be expanded as a geometric series: $D(s) = \sum_{n=0}^{\infty}(\kappa_-/\kappa_+)^{2n} e^{-2sln/k}$. Thus, collecting the exponentials into $B_j = e^{-s(x+2l(n+1)/k)} A_j$, we may write:

$$e^{-sx}\tilde{\eta}_R^-(s) = \sum_{n=0}^{\infty} \frac{\kappa_-^{2n}}{\kappa_+^{2n+2}}\left(\sum_{j=1}^{5} a_j B_j(s,x)\right), \quad (18a)$$

$$B_1 = \int_0^{\infty} e^{-s(y+x+2nl/k)} f(y)dy, \quad (18b)$$

$$B_2 = \int_0^{\infty} e^{-s(y+x+2l(n+1)/k)} f(y)dy, \quad (18c)$$

$$B_3 = \int_{-l}^{0} e^{-s(-y/k+x+2nl/k)} f(y)dy, \quad (18d)$$

$$B_4 = \int_{-l}^{0} e^{-s(y/k+x+2l(n+1)/k)} f(y)dy, \quad (18e)$$

$$B_5 = \int_{-\infty}^{-l} e^{-s(-y+x+2l(n+1)/k-l\kappa_+/k)} f(y)dy. \quad (18f)$$

Applying appropriate changes of variables, these integrals become:

$$B_1 = \int_{x+2nl/k}^{\infty} e^{-st} f(t - x - 2nl/k)dt, \quad (19a)$$

$$B_2 = \int_{x+2l(n+1)/k}^{\infty} e^{-st} f\left(t - x - \frac{2l(n+1)}{k}\right)dt, \quad (19b)$$

$$B_3 = k\int_{x+2l(n+1)/k}^{x+2nl/k} e^{-st} f(k(x-t) + 2nl)dt, \quad (19c)$$

$$B_4 = k\int_{x+2nl/k}^{x+\frac{2l(n+1)}{k}} e^{-st} f(kt - kx - 2ln - 2l)dt, \quad (19d)$$

$$B_5 = \int_{x+l(2n+k)/k}^{\infty} e^{-st} f\left(x - t + \frac{l(2n+\kappa_-)}{k}\right)dt \quad (19e)$$

Now, because the limits of integration are all positive for $x > 0$ (in region R), we can rewrite these integrals as Laplace Transforms:

$B_1 = \mathcal{L}[f(b_1)\theta(b_1)]$;
$b_1 = t - x - 2nl/k$, (20a)
$B_2 = \mathcal{L}[f(b_2)\theta(b_2)]$;
$b_2 = t - x - 2l(n+1)/k$, (20b)
$B_3 = k\,\mathcal{L}\left[f(b_3)\left(\theta(-b_3 - 2l) - \theta(-b_3)\right)\right]$;
$b_3 = k(x-t) + 2nl$, (20c)
$B_4 = k\,\mathcal{L}\left[f(b_4)\left(\theta(b_4 + 2l) - \theta(b_4)\right)\right]$;
$b_4 = k(t-x) - 2l(n+1)$, (20d)
$B_5 = \mathcal{L}\left[f(b_5)\theta\left(-b_5 - l(2 - 1/k)\right)\right]$;
$b_5 = x - t + l(2n + \kappa_-)/k$, (20e)

where $\theta(z)$ is the Heaviside Step Function. So, noting that $\tilde{\eta}_R(x,s) - \frac{1}{2}e^{-sx}\tilde{\eta}_R^-(s) = \frac{1}{2}\mathcal{L}[f(x+t) + f(x-t)\theta(x-t)]$, the inverse Laplace Transform $\mathcal{L}^{-1}[\tilde{\eta}_R]$ can be applied automatically. Thus, the solution for region R in the time domain is:

$$\eta_R(x,t) = \frac{1}{2}f(\xi_R) + \frac{1}{2}f(\nu_R)\theta(\nu_R) + \frac{1}{2(1+k)^2}\eta_R'(\nu_R); \quad (21)$$

$\eta_R'(\nu) = \sum_{n=0}^{\infty}\left(\frac{1-k}{1+k}\right)^{2n}\sum_{j=1}^{5} g_j F_j^R(h_{jn}^R(\nu))$;
$F_1^R(h) = f(h)\theta(-h-l)$; $h_{1n}^R(\nu) = \nu + \frac{l(2n+1-k)}{k}$;
$F_2^R(h) = f(h)\theta(h)$; $h_{2n}^R(\nu) = -\nu - 2nl/k$;
$F_3^R(h) = F_2^R(h)$; $h_{3n}^R(\nu) = h_{2n}^R(\nu) - 2l/k$;
$F_4^R(h) = f(h)\theta(h+l)\theta(-h)$; $h_{4n}^R(\nu) = k\nu + 2nl$;
$F_5^R(h) = f(h)\theta(-h-l)\theta(h)$; $h_{5n}^R(\nu) = -h_{4n}^R(\nu) - 2l$,

where $g_1 = 4k$, $g_2 = 1 - k^2$, $g_3 = -g_2$, $g_4 = 2k(1+k)$, and $g_5 = 2k(1-k)$. Coordinates $\nu_R(x,t) = x - t$ and $\xi_R(x,t) = x + t$ are the characteristic lines in region R.

A similar procedure can be used to find the wave disturbance height in region L:

$$\eta_L(x,t) = \frac{1}{2}f(\nu_L) + \frac{1}{2}f(\xi_L)\theta(-\xi_L - l) + \frac{\eta_L'(\xi_L)}{2(1+k)^2}; \quad (22)$$

$\eta_L'(\xi) = \sum_{n=0}^{\infty}\left(\frac{1-k}{1+k}\right)^{2n}\sum_{j=1}^{5} g_j F_j^L(h_{jn}^L(\xi))$;
$F_1^L(h) = f(h)\theta(h)$; $h_{1n}^L(\xi) = \xi - \frac{l(2n+1-k)}{k}$,
$F_2^L(h) = f(h)\theta(-h-l)$; $h_{2n}^L(\xi) = -\xi + 2nl/k - 2l$;
$F_3^L(h) = F_2^L(h)$; $h_{3n}^L(\xi) = h_{2n}^L(\xi) + 2l/k$;
$F_4^L(h) = f(h)(\theta(-h) - \theta(-h-l))$; $h_{4n}^L(\xi) = kh_{1n}^L(\xi)$;
$F_5^L(h) = f(h)(\theta(h) - \theta(h+l))$; $h_{5n}^L(\xi) = -h_{4n}^L(\xi)$;

where $\nu_L = x - t$ and $\xi_L = x + t$. Finally, for region M:

$$\eta_M(x,t) = \frac{1}{2}f(\nu_M)\theta(\nu_M + l) + \frac{1}{2}f(\xi_M)\theta(-\xi_M - l) + \frac{1}{2(1+k)^2}\left(\eta_M'^{,\nu}(\nu_M) + \eta_M'^{,\xi}(\xi_M)\right); \quad (23)$$

$\eta_M'^{,\nu}(\nu) = \sum_{n=0}^{\infty}\left(\frac{1-k}{1+k}\right)^{2n}\sum_{j=1}^{4} g_j^{M,\nu} F_j^{M,\nu}\left(h_{jn}^{M,\nu}(\nu)\right)$
$F_1^{M,\nu}(h) = f(h)\theta(h)$; $h_{1n}^{M,\nu}(\nu) = -\frac{\nu + 2nl + 2l}{k}$;
$F_2^{M,\nu}(h) = f(h)\theta(-h-l)$; $h_{2n}^{M,\nu}(\nu) = -h_{1n}^{M,\nu}(\nu) - \frac{l(1+k)}{k}$;
$F_3^{M,\nu}(h) = f(h)\theta(h+l)\theta(-h)$; $h_{3n}^{M,\nu}(\nu) = kh_{1n}^{M,\nu}(\nu)$;
$F_4^{M,\nu}(h) = f(h)\theta(-h-l)\theta(h)$; $h_{4n}^{M,\nu}(\nu) = -kh_{1n}^{M,\nu}(\nu)$;
$g_1^{M,\nu} = -2(1-k)$; $g_2^{M,\nu} = 2(1+k)$; $g_3^{M,\nu} = -(1-k^2)$;
$g_4^{M,\nu} = -(1-k)^2$;
$\eta_M'^{,\xi}(\xi) = \sum_{n=0}^{\infty}\left(\frac{1-k}{1+k}\right)^{2n}\sum_{j=1}^{4} g_j^{M,\xi} F_j^{M,\xi}\left(h_{jn}^{M,\xi}(\xi)\right)$
$F_1^{M,\xi}(h) = f(h)\theta(-h-l)$; $h_{1n}^{M,\xi}(\xi) = -\frac{\xi - 2nl - l + kl}{k}$;

$F_2^{M,\xi}(h) = f(h)\theta(h)$; $h_{2n}^{M,\xi}(\xi) = -h_{1n}^{M,\xi}(\xi) - l + l/k$;
$F_3^{M,\xi}(h) = f(h)\theta(h+l)\theta(-h)$; $h_{3n}^{M,\xi}(\xi) = -kh_{2n}^{M,\xi}(\xi)$;
$F_4^{M,\xi}(h) = f(h)\theta(-h-l)\theta(h)$; $h_{4n}^{M,\xi}(\xi) = kh_{2n}^{M,\xi}(\xi)$;
$g_1^{M,\xi} = g_1^{M,\nu}$; $g_2^{M,\xi} = g_2^{M,\nu}$; $g_3^{M,\xi} = g_3^{M,\nu}$;
$g_4^{M,\xi} = -(1+k)^2$,

where $\nu_M = x - kt$ and $\xi_M = x + kt$.

WAVE DYNAMICS

To simulate the propagation of tsunami-type solitary waves, an initial, stationary waveform is taken to be $f(x) = e^{-(x-d)^2}$ for some $d > 0$. Figures 2 and 3 exemplify several dynamical features contained in the analytical solution (21)-(23). Figure 2 is a density plot that shows the intensity of the wave as it travels along its characteristic lines. Figure 3 gives the position and profile of the wave at several times in the propagation. From Fig. 2, the initial wave at $t = 0$ splits into a right-moving wave with a peak traveling along the characteristic line $\nu_R = x - t = d$ and a left-moving wave moving along $\xi_R = x + t = d$, as in equation (21). This can be seen in Fig. 3, in which a single wave at $t = 0$ has since split into two separate waves by $t = 3$. At $t = d$, the wave has arrived at the obstacle. As it rises onto the step at the left, another characteristic line of $\nu_R = x - t = -d$ pointing to the right is seen to be generated in Fig. 2. This additional characteristic can be seen in Fig. 3, since, by $t = 4$, a third wave has been generated by the initial wave reflecting against the obstacle. The relative height of this wave has been first calculated analytically by Lamb [3] to be $R = (1-k)/(1+k)$. This can be seen from equation (21), since this wave is the first term in the infinite series ($n = 0$) with coefficient $g_2 = (1-k)(1+k)$ and overall coefficient agreeing with that of Lamb. The transmitted wave has been amplified by a transmission coefficient of $T = 2/(1+k)$ [3]. Indeed, this form of seafloor being contains the infinitely long shelf as a special case for $l \to \infty$. As the wave moves off the obstacle ($t = 4$ in Fig. 3), the wave undergoes another reflection as it encounters the second boundary. From the density plot Fig. 2 and at $t = 6$ for Fig. 3, the reflected wave in this case developed negative amplitude. From Fig. 2, this wave traverses back across the obstacle, transmits to region R $x > 0$, and again reflects off the boundary. After each reflection, the wave "trapped" on the obstacle undergoes amplitude reduction as it transmits off the obstacle at each boundary. That this process continues indefinitely is a result of the infinite series in equations (21)-(23) generating new waves and new characteristic paths at each encounter with the boundaries.

CONCLUSIONS

An analytical solution was obtained for linear water wave propagation over a symmetric underwater obstacle for a given initial stationary waveform. The solution, valid for a general initial waveform, can be directly applied to model tsunami-type solitary waves. The solution was obtained using the method of Laplace Transforms. The wave equation in each region was solved in the frequency domain, and the matched solutions were transformed back into the time domain. For a solitary waveform, the wave dynamics agree with those of an infinite length obstacle obtained in previous studies. Moreover, by taking the finiteness of the obstacle into account, other effects on propagation can be seen, including the "trapping" of a portion of the initial amplitude on top of the obstacle by internal reflections at the obstacle boundaries.

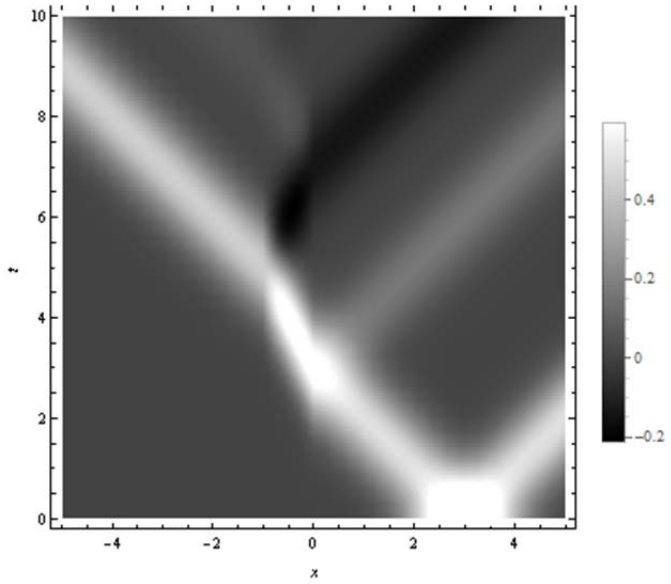

Figure 2 Density plot of wave elevation height (21)-(23) for $l = 1$, $k = 0.5$, and $d = 3$. The plot legend indicates the height of the wave.

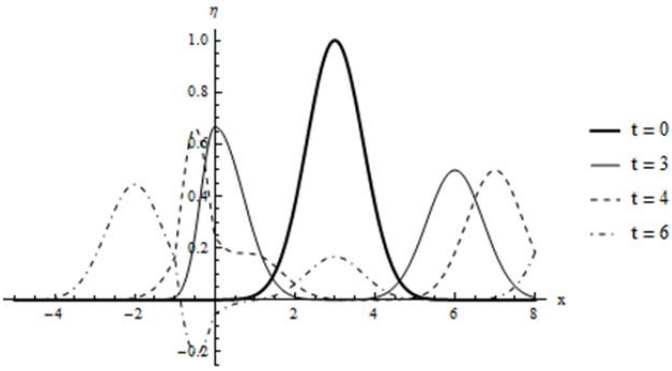

Figure 3 Portraits of the wave propagation at times $t = 0, 3, 4,$ and 6 for the same parameters as in Fig. 2.

Acknowledgments
This research was funded by the NSF award DMS-1156612.

REFERENCES

[1] Ferreira, Ó., Dias, J. A., & Taborda, R. (1994). Wave energy dissipation on a high energy barred nearshore: a natural and effective coastal protection. *Proceedings of Littoral* 1994, *EUROCOAST*, 369-379.

[2] Synolakis, C. E., & Bernard, E. N. (2006). Tsunami science before and beyond Boxing Day 2004. *Philosophical Transactions of the Royal Society A: Mathematical, Physical and Engineering Sciences*, 364(1845), 2231-2265.

[3] Lamb, H., 1932. Hydrodynamics, 6th ed. Dover, New York.

[4] Bartholomeusz, E. F. (1958, January). The reflexion of long waves at a step. In *Mathematical Proceedings of the Cambridge Philosophical Society* (Vol. 54, No. 01, pp. 106-118). Cambridge University Press.
[5] Tuck, E. O. (1977). Some classical water-wave problems in varying depth. In *Waves on Water of Variable Depth* (pp. 9-20). Springer Berlin Heidelberg.
[7] Newman, J. N. (1965). Propagation of water waves past long two-dimensional obstacles. *J. Fluid Mech*, 23(1), 23-29.
[8] Miles, J. W. (1967). Surface-wave scattering matrix for a shelf. *J. Fluid Mech, 28*(1), 755-767.
[9] Mei, C. C., & Black, J. L. (1969). Scattering of surface waves by rectangular obstacles in waters of finite depth. *Journal of Fluid Mechanics*, 38(03), 499-511.
[10] Lee, J. J., & Ayer, R. M. (1981). Wave propagation over a rectangular trench. *Journal of fluid mechanics, 110*, 335-47.
[11] Kirby, J. T., & Dalrymple, R. A. (1983). Propagation of obliquely incident water waves over a trench. *Journal of Fluid Mechanics*, 133, 47-63.
[12] Lin, P., & Liu, H. W. (2005). Analytical study of linear long-wave reflection by a two-dimensional obstacle of general trapezoidal shape. *Journal of engineering mechanics*, 131(8), 822-830.
[13] Xie, J. J., Liu, H. W., & Lin, P. (2011). Analytical Solution for Long-Wave Reflection by a Rectangular Obstacle with Two Scour Trenches. *Journal of Engineering Mechanics*, 137(12), 919-930.
[14] Whitham, G. B. (2011). *Linear and nonlinear waves* (Vol. 42). John Wiley & Sons.